



Adsorptive removal of Biochanin A, an endocrine disrupting compound, from its aqueous solution by synthesized zeolite NaA

Nitin Goyal, Sanghamitra Barman*, Vijaya Kumar Bulasara

Department of Chemical Engineering, Thapar University, Patiala 147004, Punjab, India, Tel. +91 9041933709; email: nitin.goyalgates@gmail.com (N. Goyal), Tel. +91 9878614010; email: sbarman@thapar.edu (S. Barman), Tel. +91 8437166806; email: vkbulasara@thapar.edu (V.K. Bulasara)

Received 11 March 2015; Accepted 12 October 2015

ABSTRACT

Waterborne isoflavone Biochanin A and its metabolites are known to elicit estrogenic effects in fish and affect their reproductive function. In the present investigation for the effective removal of this isoflavone, a novel zeolite NaA was synthesized, characterized, and employed for the adsorption of Biochanin A in aqueous solutions. A nanocrystalline zeolite NaA was synthesized at room temperature (25°C) via hydrothermal method without using any organic template. The synthesized zeolite was characterized by X-ray diffraction, scanning electron microscopy, and Brunauer–Emmett–Teller (BET) methods. Results showed that 72 h of aging time is needed for achieving high surface area, pore volume, and small crystal size. For the removal of Biochanin A, 1 mg/L initial concentration of Biochanin A, 1 g/L of adsorbent, pH 8, and 250 rpm stirrer speed were found to be optimum. The spectrophotometric technique was adopted for the measurement of concentration of Biochanin A in an aqueous solution. It was found that the adsorption of Biochanin A onto zeolite NaA is endothermic and the synthesized adsorbent exhibited very high removal efficiency in comparison with a commercial microporous zeolite A. Experimental data fitted well with the Langmuir isotherm and pseudo-second-order kinetic model.

Keywords: Zeolite; Adsorption; Phytoestrogen; Biochanin A; Wastewater

1. Introduction

Over the last few decades, the endocrine-disrupting compounds became a major issue in environmental chemistry due to their occurrence in environment affecting both wildlife and humans [1]. These EDCs can function as hormone mimics when released into the environment, altering natural endocrine signaling in wildlife [2]. The main source of Biochanin A is Fabaceae plants such as clover, alfalfa, peas, and soy [3]. It is

known that even at very low concentrations (a few ng/L), they cause estrogenic response in reproductive systems [4,5]. Phytoestrogens like Biochanin A and its metabolite Genistein have estrogenic effect in brown trouts, zebrafish, and *Salmo trutta* [6]. Feminization of male fish has also been observed in wastewater streams from dairy farms, soy industries, paper and pulp mills including biofuel refineries [7,8]. In fact, it was reported that the conventional wastewater treatment plants, which are mainly based on activated sludge systems are not effective in removing estrogens completely, because of their relatively high stability [9–11].

*Corresponding author.

At present, reverse osmosis (RO) and nanofiltration (NF) are considered feasible. RO particularly results in lower removal of phytoestrogens than it might be expected [12]. To achieve satisfactory removal of EDCs, further advanced treatment is needed. Adsorption and chemical advanced oxidation can be used for the advanced removal of EDCs [13]. Adsorption has been found to be superior in terms of ease of operation, initial cost, and the lack of possibility of producing secondary harmful substances. However, use of an efficient adsorbent is crucial in the case of adsorption technique guaranteeing the treatment efficiency for wastewater. The focus of the present study is therefore to synthesize a potential zeolite that can be used as an adsorbent for the removal of endocrine-disrupting compound Biochanin A (BCA) from wastewater. However, the reduction in particle size of the zeolites from micrometer to nanometer size range gives rise to dramatic changes in their properties, and subsequently the performance of the zeolites in traditional applications such as sorption significantly increases [14,15].

Various types of nanometer-sized zeolites, including NaA, faujasite-X, Y, ZSM-5, and silicalite-1, have been synthesized by hydrothermal procedures using clear aluminosilicate solutions in the presence of organic templates [16–20]. Recently, Pan et al. [19] reported the synthesis of zeolite NaA nanocrystals in a two-phase liquid segmented microfluidic reactor using a manipulated organic template-free system. However, the application of the organic templates has several disadvantages. They are costly, non-recyclable, and they require calcinations which results in pollution problems [18]. The crystallization at a moderate temperature has a pronounced effect on the ultimate zeolite crystal size. In the present investigation, the smallest size crystals of zeolite NaA synthesized by organic template-free condition has been used in sorption of Biochanin A, an endocrine-disrupting compound.

2. Materials and methods

Fumed silica, sodium hydroxide, sodium aluminate, and deionized water were used for zeolite NaA synthesis. Biochanin A and distilled water were used for the preparation of Biochanin A standard solutions. All the chemicals were procured from Sigma, MO, USA and Himedia, Mumbai, were of highest analytical grade available.

2.1. Synthesis of zeolite NaA

Zeolite NaA was synthesized by following standard procedure available in the literature [21]. Known

amounts of fumed silica (50 g/L) and NaAlO_2 (80 g/L) were dissolved in two separate flasks containing equal amounts of NaOH solutions (156 g/L). Then the two solutions were mixed in a polypropylene bottle and cured in a shaking incubator under constant stirring of 250 rpm at a temperature of $25 \pm 2^\circ\text{C}$. Samples were collected at regular intervals of time between (0 and 72 h) to study the effect of aging time on crystallization and other physical properties. The zeolite particles were separated by centrifugation (17,000 rpm, 30 min) washed several times with distilled water until the pH value dropped to 8.5 and dried in an oven at 110°C for about 12 h.

2.2. Characterization of synthesized zeolite NaA

Fig. 1 shows the scanning electron microscopy (SEM) and TEM images of synthesized zeolite NaA (72 h aging). These pictures reveal that the synthesized adsorbent was an aggregation of cubic zeolite crystals with dimensions up to $0.400 \mu\text{m}$ (average size: 300 nm). The average particle sizes of the zeolite at different aging times are shown in Table 1. The crystalline phase(s) in the materials were identified by powder X-ray diffraction (XRD) analysis on X-ray diffractometer using a Ni-filtered $\text{Cu K}\alpha$ radiation (40 kV, 40 mA) and are shown in Fig. 2. This figure shows that the growth of crystalline phases of zeolite increases with aging time (from 24 to 72 h) and the crystallization is complete in 72 h. No changes were noticed after this aging time (figure not shown). The XRD pattern of synthesized zeolite NaA for an aging time of 72 h exactly matched with the simulated XRD pattern available in the literature [22]. The three digits of the numbers mentioned above each of the peak correspond to their h , k , and l values. For some peaks, where four digits are shown, the first two digits correspond to the h value. Reduction of peak heights is due to the reduction of crystal size in the synthesized zeolite NaA.

The pore volume and surface area of the synthesized zeolite NaA were determined from N_2 adsorption–desorption measurements (shown in Fig. 3). The form of the obtained plot showed a hysteresis phenomenon indicating the presence of mesopores in the NaA zeolite. The surface area and pore volume of zeolite NaA at different aging times are shown in Table 1. The surface area of the resulting zeolite increased from 54 to $76 \text{ m}^2/\text{g}$ with an increase in the aging time (from 24 to 72 h). In a similar way, the pore volume also increased with increasing the aging time. Therefore, the zeolite NaA prepared using an optimum aging time of 72 h was used for all adsorption experiments.

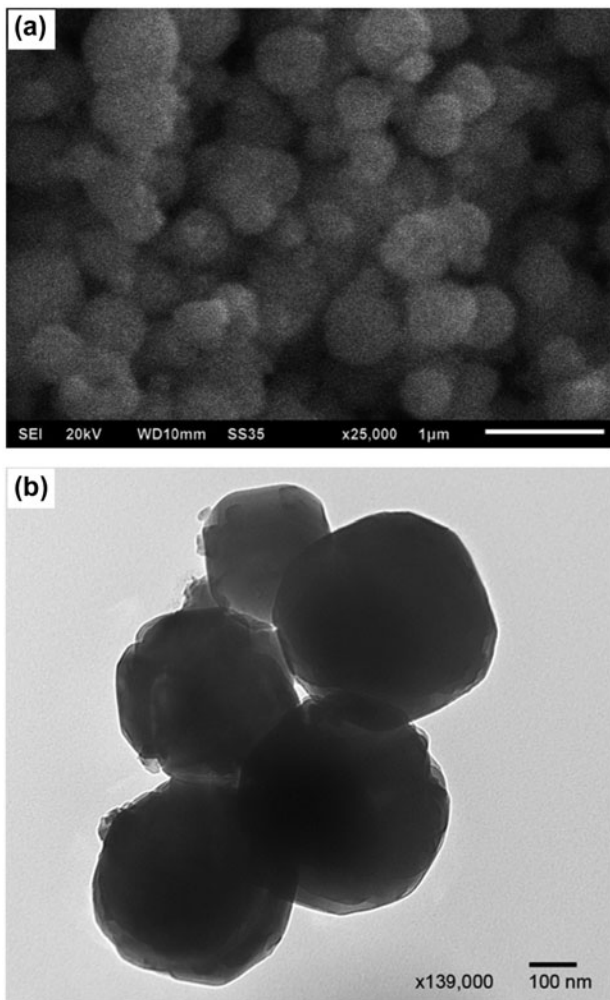


Fig. 1. (a) SEM and (b) TEM images of synthesized zeolite NaA (aging period: 72 h).

Table 1
Physical properties of the zeolite NaA synthesized using different aging times

Property	Aging time		
	24 h	48 h	72 h
SiO ₂ /Al ₂ O ₃ ratio	1:2	1:2	1:2
Average particle size from TEM (nm)	450	350	300
Pore volume (cm ³ /g)	0.04	0.11	0.13
Surface area (m ² /g)	54	68	76

2.3. Preparation of aqueous solution

Stock solution of Biochanin-A (Chemical formula: C₁₆H₁₂O₅, M.W.: 284.26 g/mol) was prepared by dissolving 10 mg in 1 L of distilled water to give concentration of 10 ppm. The serial dilute solutions of 1, 2, 3,

and 4 ppm were made by diluting the stock solution in accurate proportions. Calibration curve for Biochanin A (at a wavelength of 260 nm) was prepared by measuring the absorbance of different concentrations of the Biochanin A. The chemical structure of Biochanin A is shown in Fig. 4.

2.4. Adsorption studies

Adsorption experiments were carried out in a shaking incubator (Bionics orbital) at 250 rpm. Adsorption was performed by placing 1 g/L of adsorbent in 50 ml Biochanin A solution in a 250-ml conical flask at various concentrations. The experiments were carried out at different pH (2, 4, 6, 8, 10, and 12) and temperature range (20–50°C). The solution pH was adjusted with NaOH or HCl solutions using a pH meter (Thermo Scientific). The absorbance of Biochanin A solutions (at a wavelength of 260 nm) was determined using a UV–vis spectrophotometer (Hach, DR 5000), from which, the concentration was found through a calibration curve. Adsorption data obtained from the effect of initial concentration and contact time were used in testing the applicability of isotherm and kinetic equations, respectively.

3. Results and discussion

3.1. Adsorption of Biochanin A over zeolite NaA

3.1.1. Effect of pH on removal of Biochanin A over zeolite NaA

The pH of the solution has been reported to be an important factor in adsorption processes [23]. The variation in percent removal and adsorption capacity of zeolite NaA with solution pH is shown in Fig. 5 (Reaction conditions: C_i = 1 mg/L, T = 30°C, ω = 250 rpm). From this figure, it could be inferred that the adsorption of Biochanin A (BCA) on zeolite NaA is strongly dependent on pH values. The removal of BCA increased from 72.5% (pH 2) to 92% (pH 8) and then decreased to 65% (pH 12) and the maximum adsorption capacity was noticed at pH 8. Therefore, the optimum pH for removal of Biochanin A was chosen to be 8.

3.1.2. Effect of temperature on removal of Biochanin A over zeolite NaA

Fig. 6 shows the variation of BCA removal and adsorption capacity of zeolite NaA with temperature (Reaction conditions: C_i = 1 mg/L, pH 8, ω = 250 rpm). An increase in temperature (from 20 to 50°C) caused a

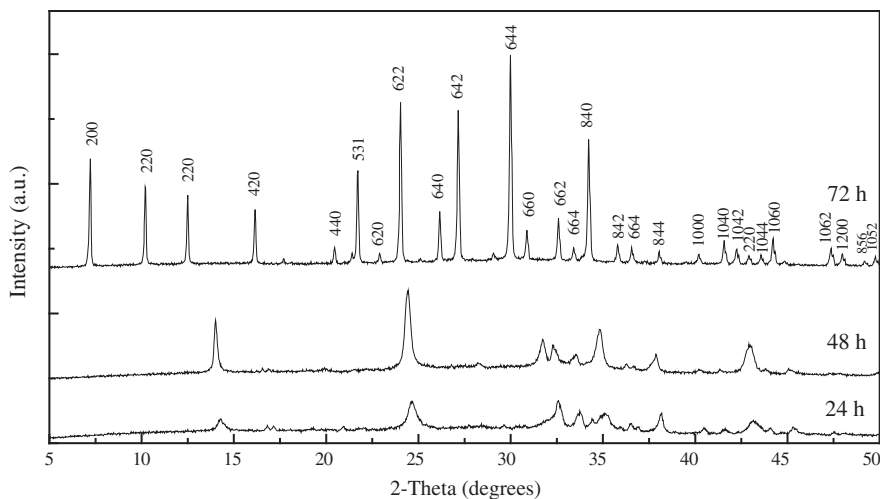


Fig. 2. XRD pattern of zeolite NaA synthesized at different aging times.

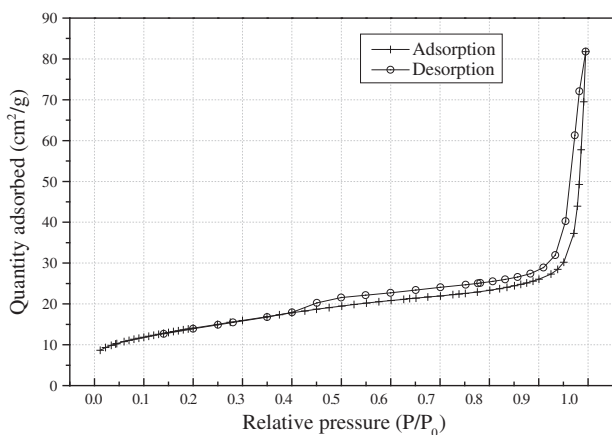


Fig. 3. N₂ adsorption–desorption isotherms of zeolite NaA (aging period: 72 h).

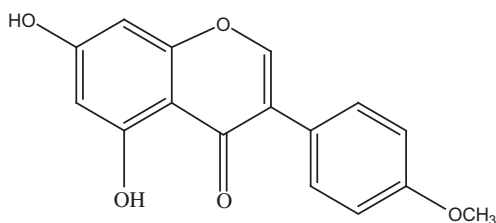


Fig. 4. Chemical structure of Biochanin A.

similar increase in BCA removal (from 46 to 78%). The mobility of BCA molecules increases with raising the temperature, and increasing temperature also produces a swelling effect within the internal structure of the zeolite (leading to widening of pores) enabling

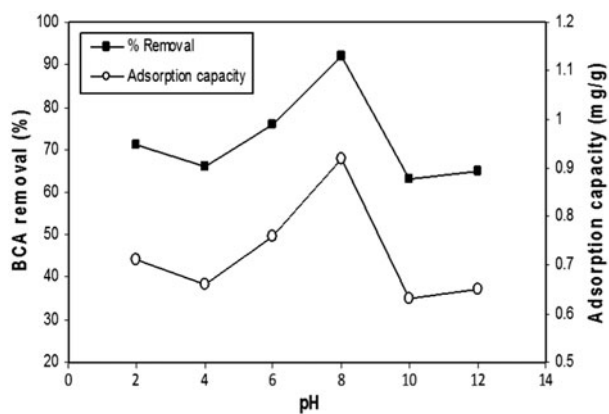


Fig. 5. Effect of solution pH on removal of Biochanin A (BCA).

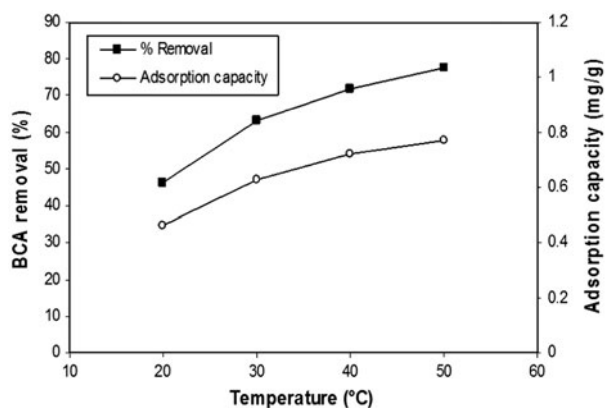


Fig. 6. Effect of temperature on removal of Biochanin A.

more phytoestrogen molecules to penetrate further. The positive effect of the temperature, wherein the adsorption capacity increased with increasing temperature, indicates that the adsorption of BCA on zeolite NaA is an endothermic process; this may be due to the enhanced rate of external and internal diffusion of the adsorbate molecules.

3.1.3. Effect of stirring on removal of Biochanin A over zeolite NaA

The effect of the agitation speed on BCA adsorption was monitored from low to moderate agitation speeds (50–300 rpm) and is shown in Fig. 7. The experiments at different shaking speeds (between 50 and 300 rpm) were carried out in a shaking incubator at 40°C and pH 8 using 1 mg/L of Biochanin A and 1 g/L of adsorbent. A maximum of 92% BCA removal was achieved at 250 rpm. Increase in agitation speed also caused increase in adsorption capacity. At high agitation, proper contact was developed between Biochanin A in solution and the binding sites of the adsorbent, which promoted effective transfer of adsorbate mass onto the adsorbent sites [23].

3.1.4. Effect of contact time on removal of Biochanin A over zeolite NaA

The effect of contact time on the adsorption of Biochanin A over zeolite NaA at room temperature ($25 \pm 1^\circ\text{C}$) is shown in Fig. 8 (reaction conditions: $C_i = 1 \text{ mg/L}$, $T = 40^\circ\text{C}$, $\text{pH} = 8$, $\omega = 250 \text{ rpm}$). The adsorption rate was observed to be rapid in the first 60 min and no further improvement was noticed after this period. Ninety-two percent removal of Biochanin A was achieved in 60 min. The fast adsorption at the initial stage was probably due to the large number of

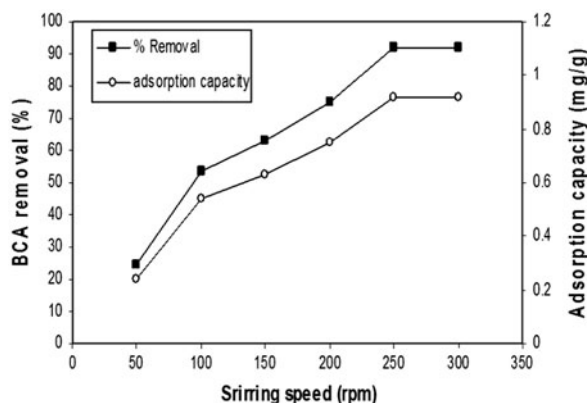


Fig. 7. Effect of stirring speed on removal of Biochanin A.

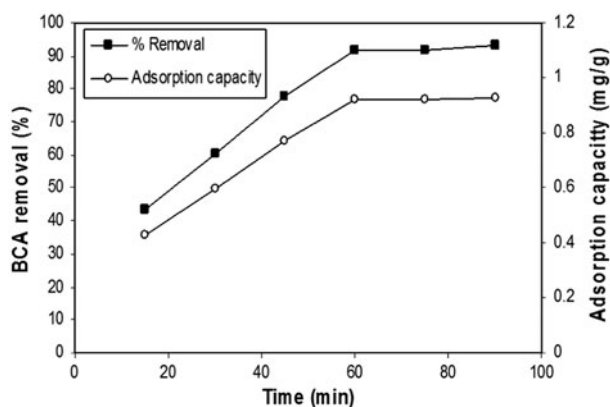


Fig. 8. Effect of contact time on removal of Biochanin A.

vacant sites available on the adsorbent surface. The attainment of equilibrium adsorption might have been due to reduction in the available active adsorption sites on the adsorbent with time resulting to limited mass transfer of the adsorbate molecules from the bulk liquid to the external surface of adsorbent.

3.1.5. Effect of adsorbent dose on removal of Biochanin A

The effect of adsorbent concentration on the removal of BCA is presented in Fig. 9 (Reaction conditions: $C_i = 1 \text{ mg/L}$, $T = 40^\circ\text{C}$, $\text{pH} = 8$, $\omega = 250 \text{ rpm}$, $t = 60 \text{ min}$). Increase in adsorbent concentration resulted in an increase in percent removal of Biochanin A. On the other hand, this has led to a substantial decrease in the adsorption capacity values. At 0.1 g/L of adsorbent dose, the removal of Biochanin A was only 31%. The maximum removal efficiency of 92.2% was achieved at an adsorbent dosage of 1 g/L. After this adsorbent

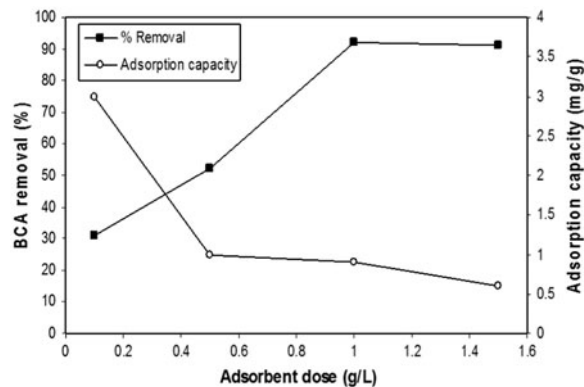


Fig. 9. Effect of adsorbent concentration on removal of Biochanin A.

dosage, the removal efficiency did not increase significantly. At high adsorbent dosages, the available Biochanin A molecules are not able to cover all the exchangeable sites on the adsorbent, resulting in constant and some slighter removal of Biochanin A. Therefore, the rest of the experiments was carried out at the adsorbent concentration of 1 g/L.

3.1.6. Effect of initial concentration of Biochanin A on its adsorption over zeolite NaA

As shown in Fig. 10, the removal efficiency of Biochanin A was strongly affected by its initial concentration (reaction conditions: $C_i = 1 \text{ mg/L}$, $C_z = 1 \text{ g/L}$, $T = 40^\circ\text{C}$, $\text{pH } 8$, $\omega = 250 \text{ rpm}$, $t = 60 \text{ min}$). Results indicated that the adsorption of Biochanin A on to zeolite NaA decreased at high solution concentration as compared to the relative values at low solution concentration. It was found that an increase in initial concentration of BCA resulted in an increase of adsorption capacity of zeolite NaA. It could be qualitatively explained by the fact that adsorption occurs initially on the available active sites of the adsorbent. At low concentration of adsorbate, the number of adsorption sites available is higher and the driving force for mass transfer is greater, which makes the adsorbate reach the adsorption site with ease. At high concentration of the adsorbate, the available adsorbent sites are limited as most of these have been occupied by adsorbate molecules causing shortage of active adsorbent sites. The maximum removal efficiency was achieved at an initial concentration of 1 mg/L, whereas, the maximum adsorption capacity (2.2 mg/g) was observed at 1 mg/L of BCA.

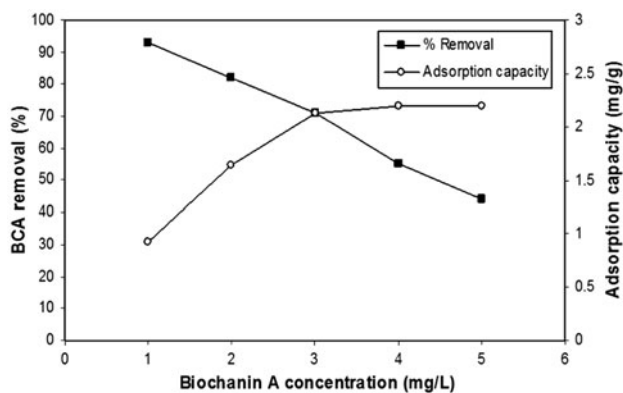


Fig. 10. Effect of initial concentration of Biochanin A on its removal.

3.2. Equilibrium studies on zeolite NaA

An adsorption isotherm describes the relationship between the amount of adsorbate that is adsorbed on the adsorbent and the concentration of dissolved adsorbate in the liquid at equilibrium. Isotherm studies were conducted at the initial pH of 8, agitation speed of 250 rpm, and a contact time of 300 min. The Langmuir isotherm equation assumes that adsorption takes place at specific homogeneous sites within the adsorbent. Once a molecule occupies a vacant site, no further adsorption can take place at that site. Moreover, the Langmuir equation is based on the assumption of a structurally homogeneous adsorbent, where all sorption sites are identical and energetically equivalent. The Langmuir isotherm model for single component adsorption is as follows:

$$q_e = \frac{Q_m K_L C_e}{1 + K_L C_e} \quad (1)$$

where q_e (mg/g) is the amount adsorbed at equilibrium, Q_m (mg/g) is the maximum adsorption capacity; and K_L (L/mg) is the Langmuir constant related to the energy of adsorption. The constant K_L represents the affinity between adsorbent and adsorbate.

The Freundlich expression is an equation based on heterogeneous surfaces suggesting that binding sites are not equivalent and/or independent [24]. The Freundlich equation is given by:

$$q_e = K_F C_e^{1/n} \quad (2)$$

The equilibrium data (C_e and q_e) obtained from the experimental study has been analyzed by the two isotherm models and the parameters thus obtained are presented in Table 2. The Langmuir isotherm parameters were obtained by fitting a straight line to the data of C_e/q_e vs. C_e and the Freundlich isotherm parameters were obtained by fitting a straight line to the data of $\ln(q_e)$ vs. $\ln(C_e)$ as shown in Fig. 11. It can be observed from Fig. 12 that the experimental data

Table 2
Model parameters of equilibrium adsorption isotherms

Langmuir isotherm model		Freundlich isotherm model	
Parameter	Value	Parameter	Value
Q_m (mg/g)	5.13	K_F [(mg/g) (L/mg) ^{1/n}]	4.66
K_L (L/mg)	13.0	$1/n$	0.054
R^2	0.9998	R^2	0.9695

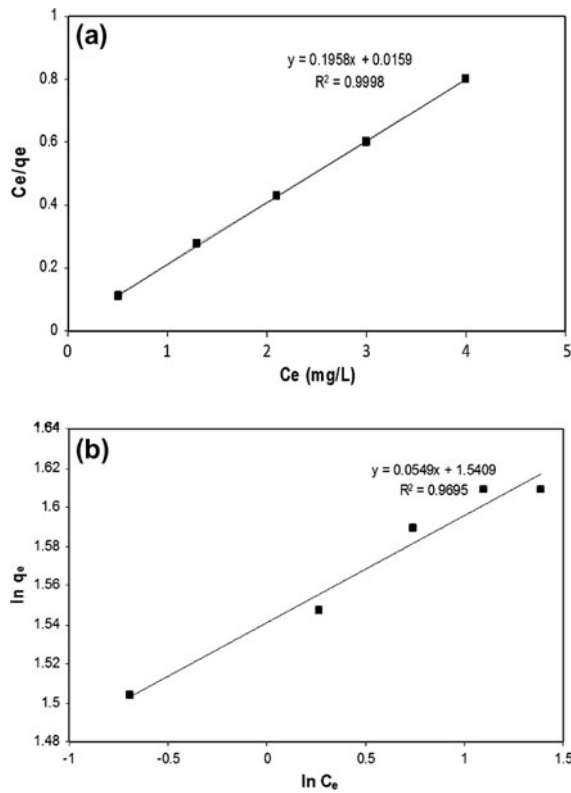


Fig. 11. Fitting of isotherm models: (a) Langmuir and (b) Freundlich.

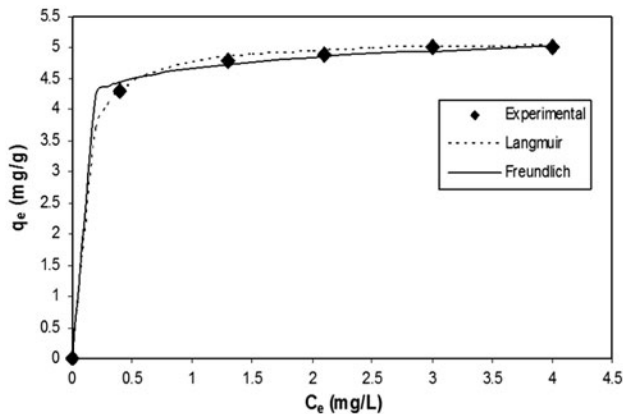


Fig. 12. Equilibrium adsorption isotherm plots for adsorption of BCA on zeolite NaA.

follow the Langmuir isotherm than the Freundlich isotherm. The model parameters presented in Table 2 also indicate that the Langmuir isotherm fits more closely ($R^2 = 0.9998$) to the experimental data and the maximum monolayer adsorption capacity of the adsorbent is 5.13 mg/g.

3.3. Adsorption kinetics

3.3.1. Pseudo-first-order model

Pseudo-first-order equation or Lagergren's kinetics equation [25] is widely used for studying the adsorption kinetics of simple adsorption systems.

$$\frac{dq_t}{dt} = k_1(q_e - q_t) \quad (3)$$

After integration and applying boundary conditions $t = 0$ to $t = t$ and $q_t = 0$ to $q_t = q_t$, the integrated form of Eq. (3) becomes:

$$-\ln\left(1 - \frac{q_t}{q_e}\right) = k_1 t \quad (4)$$

where q_t is the amount of solute adsorbed per unit of adsorbent (mg/g) at time t , k_1 is the pseudo-first-order rate constant (L/min), and t is the contact time (min). The slope of a straight line fit to the data of $-\ln(1 - q_t/q_e)$ vs. t (as shown in Fig. 13) gives the value of the rate constant, k_1 . The value of the pseudo-first-order rate constant, k_1 as obtained from the linear curve fitting is 0.0692 min^{-1} . However, the pseudo-first-order model did not yield satisfactory result as the R^2 value is very low (0.5863).

3.3.2. Pseudo-second-order model

According to the pseudo-second-order kinetic model, the rate of solute uptake is directly proportional to the square of the concentration difference of the solute from the equilibrium saturation concentration on the adsorbent. The form of rate

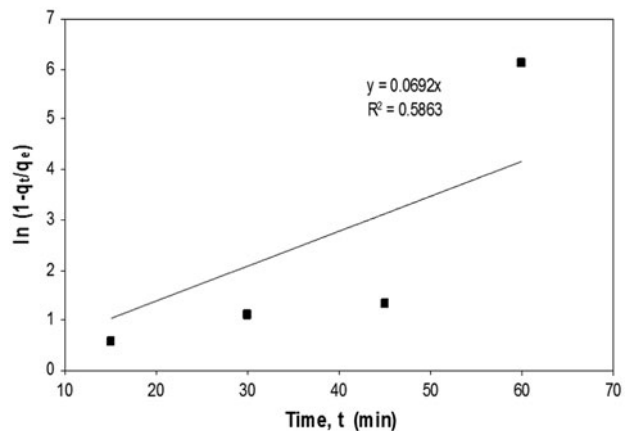


Fig. 13. Pseudo-first-order kinetic model.

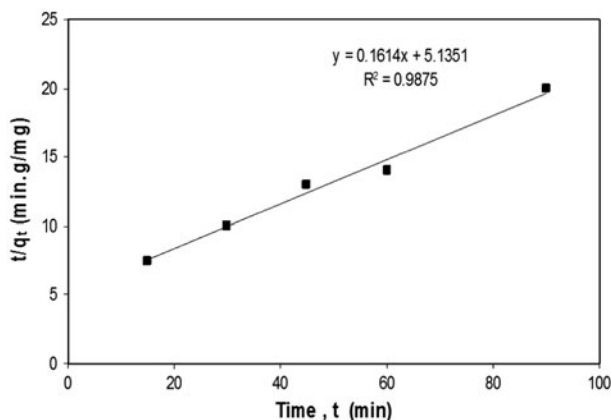


Fig. 14. Pseudo-second-order kinetic model.

equation for a pseudo-second-order kinetic model [26] is as follows:

$$\frac{dq_t}{dt} = k_2(q_e - q_t)^2 \tag{5}$$

For the boundary conditions $t = 0$ to $t = t$ and $q_t = 0$ to $q_t = q_t$, the integrated form of Eq. (5) becomes:

$$\frac{t}{q_t} = \frac{1}{k_2 q_e^2} + \frac{t}{q_e} \tag{6}$$

The values of k_2 and q_e obtained from a linear plot of t/q_t vs. t (as shown in Fig. 14) are 0.0051 g/mg min and 6.196 mg/g, respectively. It can be observed from Fig. 14 that the pseudo-second-order kinetic plot of (t/q_t) vs. (t) gave the perfect straight line fit for the adsorption of BCA onto zeolite NaA indicating that adsorption rate can be approximated by pseudo-second-order kinetic model. It is also evident from Fig. 14 that the value of the correlation coefficient is acceptable ($R^2 = 0.9875$).

3.3.3. The intra-particle diffusion model

This model considers external mass transfer (film diffusion) and internal mass transfer (pore diffusion)

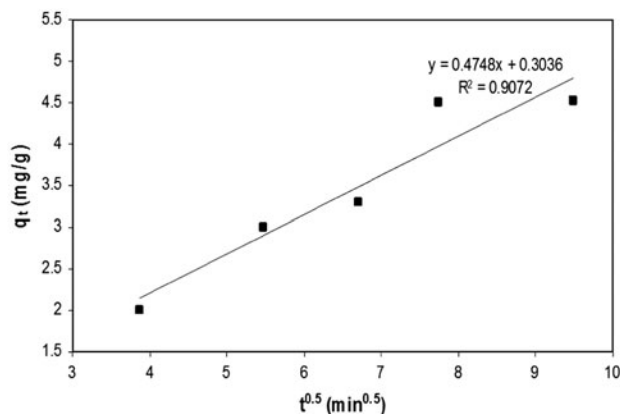


Fig. 15. Intra-particle diffusion model.

in addition to the adsorption phenomenon. The form of rate equation for the intra-particle diffusion model is as follows [27]:

$$q_t = k_1 t^{1/2} + C_1 \tag{7}$$

A straight line fit to the plot of q_t vs. $t^{0.5}$ (Fig. 15) yielded the values of k_1 and C_1 as 0.4748 mg/g min^{0.5} and 0.3036 mg/g, respectively. The R^2 value (0.9072) suggests that the model fit is reasonable.

The values of kinetic model parameters obtained from the plots are shown in Table 3. A comparison of all three kinetic models considered in this work (Table 3) indicates that the pseudo-second-order kinetic model is an appropriate model to represent the kinetic behavior of the BCA–zeolite NaA system considered in this study.

3.4. Thermodynamic study

The change in standard free energy (ΔG°) at various temperatures can be estimated as follows:

$$\Delta G^\circ = -RT \ln K_d = -RT \ln \left(\frac{q_e}{C_e} \right) \tag{8}$$

Table 3
Kinetic model parameters

Pseudo-first-order		Pseudo-second-order		Intra-particle diffusion	
Parameter	Value	Parameter	Value	Parameter	Value
k_1 (min ⁻¹)	0.0692	k_2 (g/mg min)	0.0051	k_1 (mg/g min ^{0.5})	0.4748
R^2	0.5863	q_e (mg/g)	6.196	C_1 (mg/g)	0.3036
		R^2	0.9875	R^2	0.9072

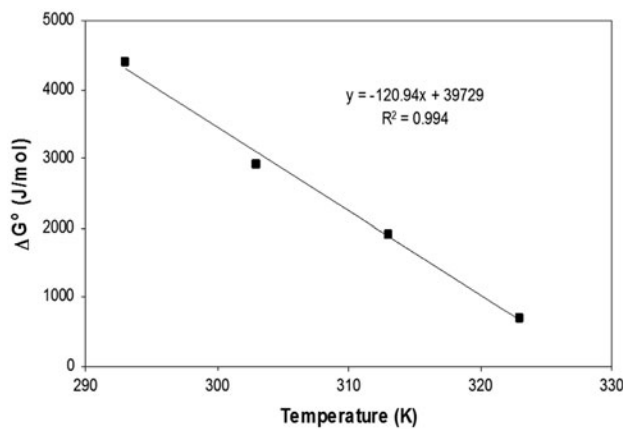


Fig. 16. Thermodynamic analysis of the experimental data.

Here R is the universal gas constant (8.314 J/mol/K), and T is the temperature in K. The relation among the thermodynamic parameters mentioned above is given by the following equation:

$$\Delta G^\circ = \Delta H^\circ - T\Delta S^\circ \quad (9)$$

A plot of ΔG° vs. T (shown in Fig. 16) yielded the values of the changes in enthalpy ($\Delta H^\circ = 39,729$ J/mol) and entropy ($\Delta S^\circ = 120.94$ J/mol K). Positive value of enthalpy change indicates the endothermic nature of the system and the positive value of entropy change indicates an increased randomness during the adsorption process.

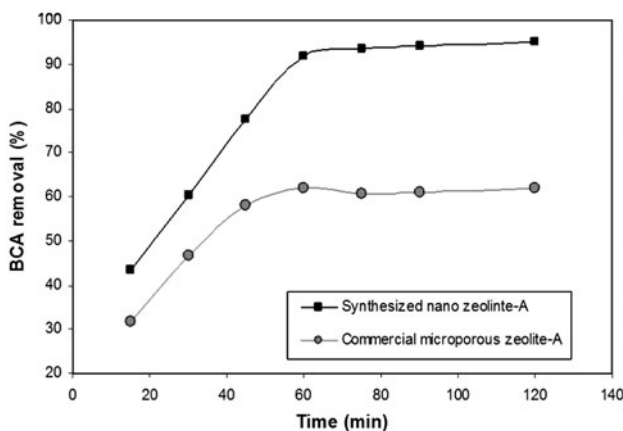


Fig. 17. Comparison of adsorption performance of the synthesized adsorbent with a commercial adsorbent.

3.5. Comparison of adsorbent performance

The adsorption performance of the synthesized zeolite NaA was compared with a commercial microporous zeolite A and is shown in Fig. 17. It can be observed that the synthesized zeolite NaA has superior adsorption capacity than the commercial adsorbent tested here. The commercial adsorbent showed a maximum removal of 62%, whereas the synthesized zeolite NaA showed 95% removal of BCA under the similar experimental conditions. Therefore, the adsorbent synthesized in this work has the potential for commercializing.

4. Conclusions

The synthesized zeolite NaA had a pore volume of $0.13 \text{ cm}^3/\text{g}$ and surface area of $76 \text{ m}^2/\text{g}$ with an average particle size of 300 nm and showed good adsorption capacity for the removal of Biochanin A (BCA), an endocrine-disrupting compound. With the simultaneous affinity toward inorganic cation and oxyanion, the synthesized zeolite NaA could be a potential adsorbent for water treatment. The synthesis process described in this work reduces the cost of synthesis by avoiding the use of expensive chemical sources as templates. Adsorption experiments conducted in batch mode indicated that the optimum pH of the BCA solution should be 8. Percent removal of BCA and adsorption capacity of zeolite NaA increased with an increase in the temperature and stirring speed and contact time. Optimum contact time was found to be 60 min. With an increase in the BCA concentration, the percent removal decreased and adsorption capacity increased. On the other hand, an increase in zeolite loading caused an increase in percent removal and decrease in adsorption capacity. The experimental data matched well with the Langmuir equilibrium isotherm and pseudo-second-order kinetic model. The adsorption process was found to be endothermic and positive value of entropy change indicated increased randomness during adsorption. In comparison with a commercial adsorbent, the synthesized zeolite NaA showed higher adsorption capacity and better removal of BCA.

Acknowledgments

This study was financially supported by research grants from the University Grants Commission (UGC), New Delhi (Grant No. 42-399/2013 (SR)) and the Department of Science and Technology (DST), New Delhi (Grant No. SB/FTP/ETA-160/2012).

Nomenclature

C_e	— equilibrium concentration of BCA in liquid phase (mg/L)
C_i	— initial concentration of BCA in liquid phase (mg/L)
C_1	— intra-particle diffusion model coefficient (mg/g)
C_z	— zeolite concentration (g/L)
k_1	— pseudo-first-order rate constant (min^{-1})
k_2	— pseudo-second-order rate constant (g/mg min)
K_F	— Freundlich Constant ((mg/g) (L/mg) ^{1/n})
K_L	— Langmuir constant (L/mg)
q_e	— amount adsorbed at equilibrium (mg/g)
Q_m	— maximum adsorption capacity (mg/g)
q_t	— amount of solute adsorbed per unit of adsorbent at time t (mg/g)
R	— universal gas constant (J/mol K)
R^2	— correlation coefficient
T	— temperature (K)
t	— time (min)
ΔG°	— standard free energy (J/mol)
ΔH°	— change in enthalpy (J/mol)
ΔS°	— change in entropy (J/mol K)
ω	— stirring speed (rpm)

References

- [1] J.P. Sumpter, Endocrine disrupters in the aquatic environment: An overview, *Acta Hydrochim. Hydrobiol.* 33 (2005) 9–16.
- [2] M.S. Lundgren, P.J. Novak, Quantification of phytoestrogens in industrial waste streams, *Environ. Toxicol. Chem.* 28 (2009) 2318–2323.
- [3] K.R. Price, G.R. Fenwick, Naturally occurring oestrogens in foods—A review, *Food Addit. Contam.* 2 (1985) 73–106.
- [4] C.E. Purdom, P.A. Hardiman, V.V.J. Bye, N.C. Eno, C.R. Tyler, J.P. Sumpter, Estrogenic effects of effluents from sewage treatment works, *Chem. Ecol.* 8 (1994) 275–285.
- [5] L.A. Racz, R.K. Goel, Fate and removal of estrogens in municipal wastewater, *J. Environ. Monit.* 12 (2010) 58–70.
- [6] H. Holbech, K.D. Schröder, M.L. Nielsen, N. Brande-Lavridsen, B.F. Holbech, P. Bjerregaard, Estrogenic effect of the phytoestrogen biochanin A in zebrafish, *Danio rerio* and brown trout, *Salmo trutta*, *Aquat. Toxicol.* 144–145 (2013) 19–25.
- [7] A. Bacaloni, C. Cavaliere, A. Faberi, P. Foglia, R. Samperi, A. Laganà, Determination of isoflavones and coumestrol in river water and domestic wastewater sewage treatment plants, *Anal. Chim. Acta* 531 (2005) 229–237.
- [8] M. Farré, M. Gros, B. Hernández, M. Petrovic, P. Hancock, D. Barceló, Analysis of biologically active compounds in water by ultra-performance liquid chromatography quadrupole time-of-flight mass spectrometry, *Rapid Commun. Mass Spectrom.* 22 (2008) 41–51.
- [9] A.C. Johnson, A. Belfroid, A.D. Corcia, Estimating steroid oestrogen inputs into activated sludge treatment works and observations on their removal from the effluent, *Sci. Total Environ.* 256 (2000) 163–173.
- [10] L. Balest, G. Mascolo, C.D. Iaconi, A. Lopez, Removal of endocrine disrupter compounds from municipal wastewater by an innovative biological technology, *Water Sci. Technol.* 58 (2008) 953–956.
- [11] Y. Wang, W. Hu, Z. Cao, X. Fu, T. Zhu, Occurrence of endocrine disrupting compounds in reclaimed water from Tianjin, China, *Anal. Bioanal. Chem.* 383 (2005) 857–863.
- [12] L.D. Nghiem, A. Manis, K. Soldenhoff, A.I. Schäfer, Estrogenic hormone removal from wastewater using NF/RO membranes, *J. Membr. Sci.* 242 (2004) 37–45.
- [13] M.S. Lundgren, Identification and Quantification of Phytoestrogens from Industrial Sources and Removal Mechanisms of Phytoestrogens during Wastewater Treatment Plant Operations, M.Sc. Thesis, University of Minnesota, US, 2009.
- [14] S. Mintova, T. Bein, Nanosized zeolite films for vapor-sensing applications, *Microporous Mesoporous Mater.* 50 (2001) 159–166.
- [15] B.O. Hincapie, L.J. Garces, Q. Zhang, A. Sacco, S.L. Suib, Synthesis of mordenite nanocrystals, *Microporous Mesoporous Mater.* 67 (2004) 19–26.
- [16] G. Zhu, S. Qiu, J. Yu, Y. Sakamoto, F. Xiao, R. Xu, O. Terasaki, Synthesis and characterization of High-quality zeolite LTA and FAU single nanocrystals, *Chem. Mater.* 10 (1998) 1483–1486.
- [17] R. Ravishankar, C. Kirschhock, B.J. Schoeman, P. Vanoppen, P.J. Grobet, S. Storck, W.F. Maier, J.A. Martens, F.C.D. Schryver, P.A. Jacobs, Physicochemical characterization of silicalite-1 nanophase material, *J. Phys. Chem. B* 102 (1998) 2633–2639.
- [18] Y. Cheng, L.J. Wang, J.S. Li, Y.C. Yang, X.Y. Sun, Preparation and characterization of nanosized ZSM-5 zeolites in the absence of organic template, *Mater. Lett.* 59 (2005) 3427–3430.
- [19] Y. Pan, M. Ju, J. Yao, L. Zhang, N. Xu, Preparation of uniform nano-sized zeolite A crystals in microstructured reactors using manipulated organic template-free synthesis solutions, *Chem. Commun.* 45 (2009) 7233–7235.
- [20] B.A. Holmberg, H. Wang, Y. Yan, High silica zeolite Y nanocrystals by dealumination and direct synthesis, *Microporous Mesoporous Mater.* 74 (2004) 189–198.
- [21] Z. Ghasemi, H. Younesi, Preparation and characterization of nano zeolite NaA from rice husk at room temperature without organic additives, *J. Nano Mater.* 2011 (2011) 858961–858968.
- [22] M.J. Treacy, J.B. Higgins, Collection of Simulated XRD Powder Patterns for zeolites, fourth ed., Elsevier, Amsterdam, 2001, p. 215.
- [23] A. Garg, M. Mainrai, V.K. Bulasara, S. Barman, Experimental investigation on adsorption of Amido Black 10B dye onto zeolite synthesized from fly ash, *Chem. Eng. Commun.* 202 (2015) 123–130.

- [24] Z.R. Holan, B. Volesky, I. Prasetyo, Biosorption of cadmium by biomass of marine algae, *Biotechnol. -Bioeng.* 41 (1993) 819–825.
- [25] A. Bhattacharya, C. Venkobachar, Removal of cadmium(II) by low cost adsorbents, *J. Environ. Eng.* 110 (1984) 110–122.
- [26] Y.S. Ho, G. McKay, Pseudo-second order model for sorption processes, *Process Biochem.* 34 (1999) 451–465.
- [27] A.K. Ojha, V.K. Bulasara, Adsorption characteristics of jackfruit leaf powder for the removal of Amido black 10B dye, *Environ. Prog. Sustainable Energy* 34 (2015) 461–470.